REGULAR ARTICLE

blood advances

Characteristics of circulating KSHV-infected viroblasts during active KSHV$^+$ multicentric Castleman disease

Gregoire Martin de Frémont,[1-3,*] Anthony Vanjak,[1-3,*] Zineb Sbihi,[1,†] Silene Knapp,[1,†] Margaux Garzaro,[1-3,†] Marwa Chbihi,[1,‡] Benjamin Fournier,[4,‡] Justine Poirot,[1,‡] Antoine Dossier,[5,‡] Marc-Antoine Silvestrini,[1] Juliette Villemonteix,[6] Véronique Meignin,[7] Lionel Galicier,[2,3] Rémi Bertinchamp,[2,3] Jerome Le Goff,[8] Maud Salmona,[8] Edouard Flamarion,[9] Charles Cassius,[10] Celeste Lebbé,[10] Anne Marie Ronchetti,[11] Sylvain Latour,[4] Eric Oksenhendler,[2,3] Guislaine Carcelain,[1] and David Boutboul[1-3]

[1]INSERM U976 HIPI, équipe INSIGHT, Institut de Recherche Saint-Louis, Université Paris Cité, Paris, France; [2]Department of Clinical Immunology, Hôpital Saint-Louis, Assistance Publique-Hôpitaux de Paris (AP-HP), Université Paris Cité, Paris, France; [3]National Reference Center for Castleman disease, Hôpital Saint-Louis, AP-HP, Université Paris Cité, Paris, France; [4]Laboratory of Lymphocyte Activation and Susceptibility to EBV Infection, INESRM UMR 1163, Imagine Institute, Université Paris Cité Paris, France; [5]Department of Internal Medicine, Hôpital Bichat, AP-HP, Université Paris Cité, Paris, France; [6]Laboratory of Immunology, Hôpital Robert Debré, AP-HP, Université Paris Cité, Paris, France; [7]Department of Pathology, Hôpital Saint-Louis, AP-HP, Université Paris Cité, Paris, France; [8]Laboratory of Virology, Hôpital Saint-Louis, AP-HP, Université Paris Cité, Paris, France; [9]Department of Internal Medicine, Hôpital Européen Georges Pompidou, AP-HP, Université Paris Cité, Paris, France; [10]Department of Dermatology, Hôpital Saint-Louis, AP-HP, Université Paris Cité, Paris, France; and [11]Department of Clinical Hematology, Centre Hospitalier Sud Francilien, Corbeil-Essonnes, France

Key Points

- Circulating KIVs are detectable during active KSHV$^+$ MCD.
- These cells differ from conventional plasmablasts, express latent and lytic viral transcripts, and display a low immunogenic profile.

Kaposi sarcoma–associated herpesvirus (KSHV)/human herpesvirus 8–associated multicentric Castleman disease (MCD) is a polyclonal B-cell lymphoproliferative disorder that mainly occurs in immunocompromised hosts. The diagnosis relies on lymph node biopsy demonstrating KSHV-infected cells located in the mantle zone with a marked interfollicular plasma cell infiltration. Infected cells are large cells positive for immunoglobulin M (IgM), λ light chain, and CD38, described initially as infected plasmablasts. We show that IgM$^+$λ$^+$CD38^{high} cells were also detectable in the peripheral blood of 14 out of 18 (78%) patients with active KSHV-MCD and absent in 40 controls. Using immunofluorescence and flow–fluorescence in situ hybridization, we demonstrate that these cells are KSHV infected and express both latent and lytic KSHV transcripts. These KSHV-infected viroblasts (KIVs) harbor a distinct phenotype compared with conventional plasmablasts. We also identified several putative mechanisms of immune escape used by KSHV, because KIVs displayed an overall decrease of costimulatory molecules, with a remarkable lack of CD40 expression and are interleukin-10–producing cells. The identification of this specific and easily accessible KSHV$^+$ circulating population brings new elements to the understanding of KSHV-MCD but also raises new questions that need to be clarified.

Introduction

Multicentric Castleman disease (MCD) is a heterogeneous entity encompassing several lymphoproliferative disorders with close histopathological patterns. One MCD subset is associated with Kaposi sarcoma (KS)–associated herpesvirus (KSHV)/human herpesvirus 8 infection and mainly affects individuals infected with HIV or those who received transplants. The course of KSHV-MCD is marked by

Submitted 29 June 2022; accepted 24 October 2022; prepublished online on *Blood Advances* First Edition 12 December 2022; final version published online 26 April 2023. https://doi.org/10.1182/bloodadvances.2022008456.

*G.M.d.F. and A.V. contributed equally to this study.

†Z.S., S.K., and M.G. contributed equally to this study.

‡M.C., B.F., J.P., and A.D. contributed equally to this study.

Presented in oral form at the 64th annual meeting of the American Society of Hematology, New Orleans, LA, 10 December 2022.

Data are available on request from the corresponding author, David Boutboul (david.boutboul@aphp.fr).

The full-text version of this article contains a data supplement.

© 2023 by The American Society of Hematology. Licensed under Creative Commons Attribution-NonCommercial-NoDerivatives 4.0 International (CC BY-NC-ND 4.0), permitting only noncommercial, nonderivative use with attribution. All other rights reserved.

Downloaded from http://ashpublications.net/bloodadvances/article-pdf/7/9/1682/2049158/blooda_adv-2022-008456-main.pdf by guest on 08 June 2024

flares causing fever, lymphadenopathy, splenomegaly, effusion, cytopenia, hypoalbuminemia, and a high serum C-reactive protein (CRP) level reflecting a high degree of systemic inflammation. KS lesions may coexist with KSHV-MCD. The cytokine storm is measurable in patients' serum with high levels of interleukin 6 (IL-6) and IL-10 during flares.[1] Life-threatening complications may occur, including hemophagocytic syndrome,[2] and KSHV-MCD is, therefore, considered a medical emergency. Lymph node biopsy and pathological examination remain the gold standards for diagnosis. KSHV-MCD is characterized by plasma cell–type MCD features with prominent polytypic interfollicular plasmacytosis and pathognomonic immunoglobulin $M^+\lambda^+$ ($IgM^+\lambda^+$) cells that are mainly located in the mantle zone and positive for the KSHV latent nuclear antigen (LNA). These KSHV-infected cells were named "plasmablasts" based on their morphology in optic microscopy.[3] These cells are $CD38^+$, $CD138^-$, and variably positive for CD27 (10% to 30%). Few cells express the B-cell markers CD79a and CD20.[4,5] Whole-blood KSHV quantification is a helpful diagnostic marker but has technical delays and lacks specificity.[6,7] It has also been found positive in other KSHV-associated diseases such as KS and primary effusion lymphoma (PEL). Available treatment options for KSHV-MCD combine the B-cell–depleting monoclonal antibody rituximab[8,9] and cytotoxic agents (liposomal doxorubicin and etoposide) for severe flares.

We first reported the evidence for circulating KSHV-infected cells during KSHV-MCD flares in 3 patients with circulating polyclonal $IgM^+\lambda^+$ plasmablastic cells.[10] At the time of that report, the phenotype of these cells was not thoroughly explored. Based on that preliminary report, we hypothesized that during KSHV-MCD flares, a circulating cell population with specific features could be detected. The easy access to these cells may help the in-depth study of KSHV-MCD.

Methods

Study design and participants

Between January 2020 and August 2021, 18 patients with KSHV-MCD flares were included from 4 secondary and tertiary care centers in the Paris, France area (Table 1). Diagnosis of KSHV-MCD flare was based on the criteria defined by Gérard et al[8] (supplemental Table 1). All cases were confirmed by lymph node samples. Post-rituximab MCD flares were defined as disease flares, as previously defined, occurring in the month after rituximab infusion. Controls included 19 patients with a history of KSHV infection (KSHV-MCD in remission, other KSHV-related diseases, or asymptomatic KSHV infection) (Table 1) and 21 patients that were $KSHV^-$ (Table 2). Antibodies against KSHV were absent in all patients that were $KSHV^-$ (assessed by immunofluorescence performed on BC-3 cell line, a $KSHV^+$ PEL-derived cell line).

Table 1. Clinical and biological characteristics of the $KSHV^+$ subgroup

	KSHV-MCD flare (n = 16)	Postrituximab KSHV-MCD flare (n = 2)*	$KSHV^+$ controls (n = 19)	*P*
Sex, male, n (%)	15 (94)	1 (50)	16 (84)	.20
Age, median (IQR), y	56 (50-67)	60 (40-79)	60 (43-72)	.91
KSHV-related diseases, n (%)				
MCD	16 (100)	2 (100)	10 (52)	**<.01**
KS	7 (44)	0	8 (42)	.75
PEL	0	0	3 (16)	.35
DLBCL	0	0	1 (5)	>.99
Asymptomatic KSHV infection	–	–	2 (11)	–
Type of immunosuppression, n (%)				
HIV^+	8 (50)	1 (50)	9 (47)	>.99
Positive HIV viral load	5 (31)	1 (50)	2 (11)	.18
Organ transplant recipient	0	0	1 (5)	>.99
Biological findings, median (IQR)				
CRP	72 (36-115)	216 (142-290)	2 (0-34)	**<.001**
KSHV viral load, log copies per mL	6.4 (5.9-6.7)	5.6 (5-6.3)	3.9 (0.7-4.7)	**<.001**
History of KSHV-related disease treatment				
Etoposide, n (%)	9 (56)	1 (50)	6 (32)	.37
Rituximab, n (%)	7 (44)	2 (100)	5 (26)	.17
Duration since last rituximab infusion, median [IQR], mo	23 (20-42)	0.4 (0.3-0.5)	13 (8-60)	.33†
Pegylated liposomal doxorubicin, n (%)	1 (6)	0	4 (21)	.51
Pembrolizumab, n (%)	2 (13)	0	2 (11)	>.99
Other treatments, n (%)	1 (6)	0	7 (37)	.08

*n = 2, [minimum-maximum]
†Postrituximab flares were not included in the statistical analysis.

Downloaded from http://ashpublications.net/bloodadvances/article-pdf/7/9/1682/2049158/blooda_adv-2022-008456-main.pdf by guest on 08 June 2024

Table 2. Clinical characteristics of the KSHV^{-} subgroup

	Post–severe acute respiratory syndrome coronavirus 2 vaccination (n = 13)	Acute infection (n = 3): malaria (n = 1), HIV (n = 1), EBV (n = 1)	Autoimmune disease (n = 2): IgG4-related disease (n = 1) and systemic lupus erythematosus (n = 1)	Healthy donors (n = 3)	*P*
Sex, male, n (%)	4 (31)	3 (100)	1 (50)	2 (67)	.15
Age, median (IQR), y	36 (30-45)	35 (33-41)	58	30 (27-30)	.25

Study approval

This study was approved by the local institutional review board (IMMUNOLYMPH protocol, CLEA-2020-113) and was conducted in accordance with the Declaration of Helsinki. All patients gave informed consent before study enrollment.

Flow cytometry phenotyping

Peripheral blood mononuclear cells (PBMCs) were isolated within 6 hours from whole-blood collection using Ficoll separation (PanBiotech), because a decrease in staining reliability was observed with postponed Ficoll separation and in frozen samples (data not shown). For surface staining, PBMCs (1×10^6 to 3×10^6 cells per sample) were washed in fluorescence-activated cell sorting (FACS) staining buffer (2% fetal calf serum in phosphate-buffered saline [PBS]) once and in PBS twice, then incubated for 30 minutes at 4°C (in the dark) with appropriate fluorochrome-labeled monoclonal antibodies or their isotype-matched control antibodies diluted in 60 µL FACS staining buffer. The gating strategy is detailed in Figure 1. Samples were acquired and analyzed using a flow cytometer (BD FACSCelesta) and FlowJo software. The following antibodies were used: anti-CD3 (HIT3a), anti-CD5 (L17F12), anti-CD14 (HCD14), anti-CD19 (HIB19), anti-CD40 (5C3), anti-CD70 (113-16), anti-CD137-L (5F4), anti-IgM (MHM88), anti–OX40-L/anti-CD252 (11C3.1), anti–ICOS-L/CD275 (2D3) (BioLegend); anti-CD20 (2H7), anti-CD24 (ML5), anti-CD27 (L128), anti-CD38 (HB7), anti-CD86 (2331), anti-CD138 (MI15), anti-κ (G20-193), anti-λ (JDC-12) (BD Biosciences); and anti–PD-L1/CD274 (MIH1) (TF Invitrogen).

Interleukin intracellular staining

PBMCs were collected from patients, as described previously, and were incubated in a culture medium (RPMI 1640 + 10% fetal calf serum) and 1000× brefeldin A (Thermo Fisher Scientific) for 6 hours. Extracellular staining was performed before fixation and permeabilization (intracellular fix/intracellular permeabilization buffer, eBioscience). Intracellular interleukins were stained with anti–human IL-6 (hIL-6) (AS12, BD Biosciences) and anti–IL-10 antibodies (JES3-9D7, eBioscience).

Immunofluorescence

Coverslips were incubated with L-polylysine for 2 hours at 37°C. PBMCs (2×10^5) were seeded on each coverslip. Cells were washed twice in PBS 30 minutes, fixed for 15 minutes in 4% paraformaldehyde, and permeabilized for 15 minutes in 0.1% Triton X-100 in PBS at room temperature. Cells were then incubated for 30 minutes with blocking buffer (5% bovine serum albumin [BSA], 0.1% fish gelatin, and 100 mM glycine at pH 7) and thereafter for 30 minutes in 5% BSA in PBS. Next, coverslips were incubated for 45 minutes with mouse anti-LNA1 (13B10, KSHV; Bio SB Diagomics) and rabbit anti-IgM (JF84-09, Invitrogen) antibodies diluted in 1% BSA-PBS. The cells were washed with PBS and incubated for 45 minutes with goat antimouse Alexa Fluor 546 (orange, Invitrogen) and goat antirabbit Alexa Fluor 488 (green, Invitrogen). Images were acquired on a Zeiss LSM800 confocal microscope and analyzed using ZEN software (Zeiss).

Flow–fluorescence in situ hybridization (flow-FISH)

The assay was performed on frozen PBMCs and on cultured cell lines (BCP1 cells, a KSHV^{+}/Epstein-Barr virus [EBV]–negative PEL-derived cell line, and an EBV-infected lymphoblastic cell line [LCL]). Cells (2×10^6 to 4×10^6) were seeded in a 96-well round-bottomed plate, washed in 150 μL of FACS staining buffer, stained for 30 minutes at 4°C (in the dark), and washed again in 150 μL of FACS staining buffer. After fixation and permeabilization, as recommended in the PrimeFlow RNA assay (eBioscience), intracellular staining of κ and λ light chains was performed. The previously cited antibodies were used and conjugated to either phycoerythrin, phycoerythrin-cyanine 7, allophycocyanin, allophycocyanin-cyanine 7, and AF700 or brilliant violet (BV) 421, BV510, BV605, BV650, BV711, and BV786. For each sample, 2 wells, each with 10^6 cells, were unstained for the first and only stained with control probes for the second (RPL13A, a positive hybridization control, and *Bacillus subtilis* dapB, a negative hybridization control), respectively. The probes used in the assay were RPL13A type 4 (Alexa Fluor 488), *Bacillus* type 1 (Alexa Fluor 647), open reading frame K2 (gene coding for the viral IL-6 [vIL-6]) type 4, and open reading frame 73 (gene coding for the LNA protein) type 10 (Alexa Fluor 568). RNA in situ hybridization was conducted as described by the manufacturer (eBioscience) using the probes and reagents of the PrimeFlow RNA assay. Analysis was performed by flow cytometry (BD FACS ARIA III).

Statistics

Patient characteristics are expressed as median (interquartile range [IQR]). Spearman correlations were evaluated using R in Rstudio (version 1.3.1093) and represented with the ggplot2 package (version 3.3.5). Mean fluorescence intensity (MFI) was analyzed with Mann-Whitney *U* test (GraphPad Prism version 9.0 software) (*$P < .05$, **$P < .01$, ***$P < .001$, ****$P < .0001$).

Results

Patient characteristics

A total of 58 subjects were enrolled in this study. The main characteristics of each group are detailed in Tables 1 and 2.

Patients with KSHV-MCD flares (n = 18). Among the 18 patients, 2 had a flare in the month after rituximab infusion

Downloaded from http://ashpublications.net/bloodadvances/article-pdf/7/9/1682/2049158/blooda_adv-2022-008456-main.pdf by guest on 08 June 2024

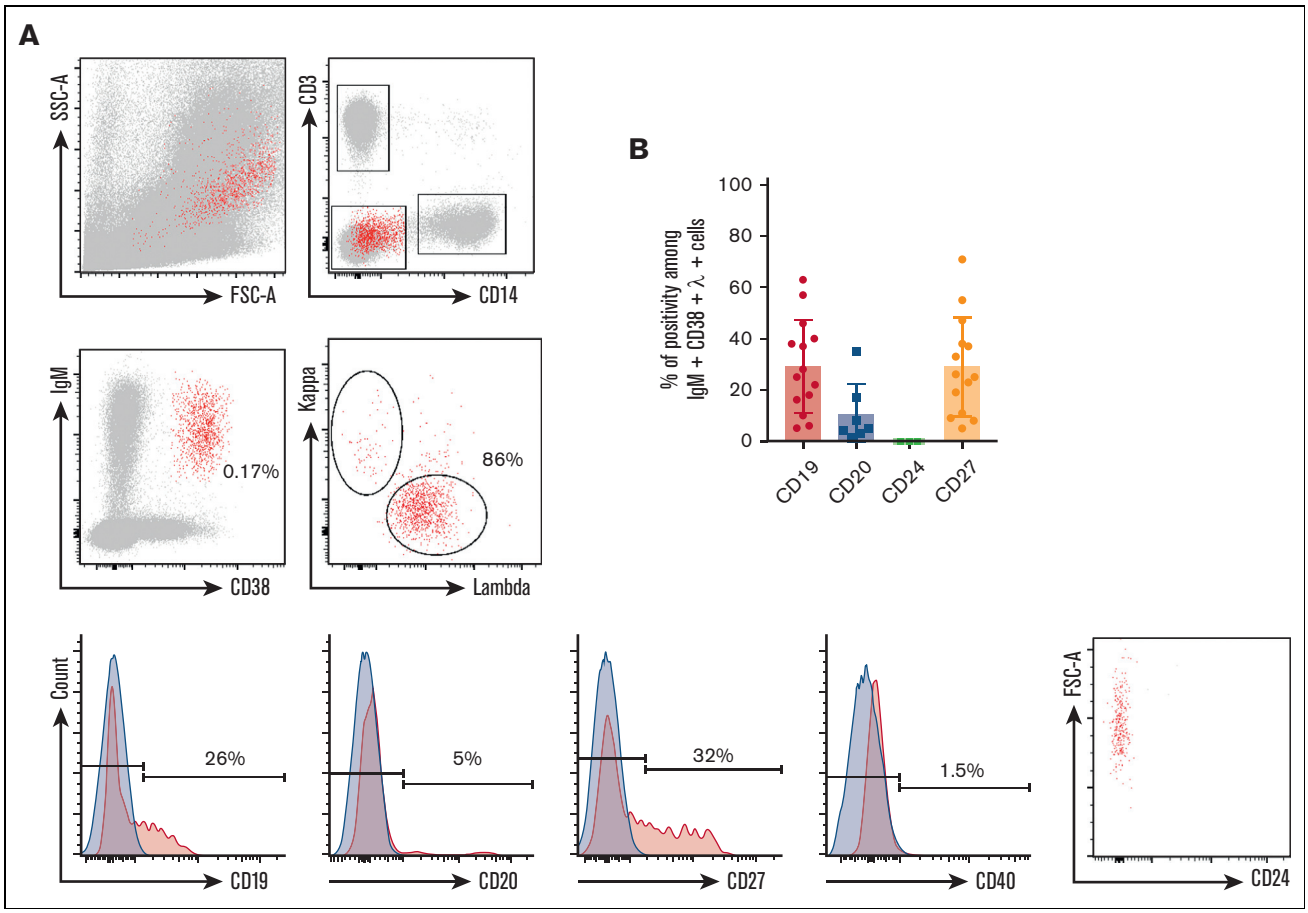

Figure 1. Phenotype of circulating IgM$^+$λ$^+$CD38^{high} cells during KSHV-MCD flare. (A) P1 PBMCs were isolated using Ficoll gradient and stained using the method described in "Material and Methods." At least 10^6 events were acquired. Gating strategy was performed as follows: (1) gating on single cells; (2) exclusion of T cells (CD3$^+$) and monocytes (CD14$^+$); (3) gating on IgM$^+$CD38^{high} cells; (4) gating on λ$^+$ cells; and (5) assessment of CD19, CD20, CD24, CD27, and CD40 expression. Retrogating of the IgM$^+$λ$^+$CD38^{high} population was performed on a side scatter/forward scatter (SSC/FSC) dot plot. Positivity threshold was determined on the fluorochrome corresponding isotype (depicted in blue). P1 is shown as a representative example. (B) Percentage of CD19, CD20, CD24, and CD27 positivity among IgM$^+$λ$^+$CD38^{high} circulating cells detected in 14 patients with KSHV-MCD.

and were analyzed separately. Among the 16 other patients, 15 (94%) were male, with a median age of 56 years (interquartile range [IQR], 50-67 years). Of these 16 patients, 9 (56%) had isolated MCD and 7 (44%) had MCD associated with cutaneous and mucosal lesions of KS. Additionally, 8 (50%) patients were infected with HIV and 5 (31%) had detectable plasma HIV RNA. The median CRP level was 72 mg/L (IQR, 36-115 mg/L) and the median whole-blood KSHV DNA was 6.4 log copies per mL (IQR, 5.9-6.3 log copies per mL). There was a significant correlation between these 2 variables (r^2 = 0.65, P < .01) (supplemental Figure 1). In total, 9 of 16 (56%) patients had a history of etoposide exposure (median, 17 months since the previous infusion; IQR, 6-22 months) and 7 of 16 (44%) had been treated with rituximab (median, 23 months since the previous infusion; IQR, 20-42 months). Pembrolizumab was administered to 2 (13%) patients for associated KS, 5 and 9 months before sampling. Furthermore, 1 (6%) patient received pegylated liposomal doxorubicin for KS 2 years before sampling and 1 (6%) received a combination of cytotoxic agents >5 years before the flare.

The 2 patients with MCD flares in the month following rituximab infusion were a 40-year-old woman with uncontrolled HIV infection and a 79-year-old man without underlying immunosuppression. Flares occurred on days 10 and 15, respectively, after the last infusion.

The 2 groups did not show differences because the 2 patients with post-rituximab KSHV-MCD flares also had elevated CRP levels and blood KSHV DNA titers.

KSHV$^+$ control group (n = 19). This group was defined by KSHV infection without criteria for KSHV-MCD flare and all patients had a positive KSHV serology. Of the 19 patients, 16 were men, with a median age of 60 years. In total, 10 patients had a history of KSHV-MCD considered as being in remission (median time of remission, 60 months), with (n = 5) or without (n = 5) associated KS, 3 had KS alone, 3 had active PEL, 1 had KSHV$^+$ diffuse large B-cell lymphoma (DLBCL), and 2 had asymptomatic KSHV infection. Asymptomatic KSHV infection was defined by a history of detectable KSHV viremia without any clinical and/or

Downloaded from http://ashpublications.net/bloodadvances/article-pdf/7/9/1682/2049158/blooda_adv-2022-008456-main.pdf by guest on 08 June 2024

biological symptoms suggestive of KSHV-associated diseases. Nine patients were infected with HIV and 1 received a kidney transplant. The median serum CRP level was 2 mg/L and the median whole-blood KSHV DNA viral load was 3.9 log copies per mL. There was no correlation between these 2 variables ($r^2 = 0.2$, $P = .42$; data not shown).

As expected, CRP levels and KSHV blood titers were significantly higher in patients with MCD flares than in the KSHV$^+$ control group ($P < .01$, Mann-Whitney U test), but no other significant differences were observed.

KSHV$^-$ control group (n = 21). Of the 21 patients, 10 were men, with a median age of 33 years. In total, 13 were healthy individuals from whom samples were taken within 2 weeks after vaccination against severe acute respiratory syndrome coronavirus 2, 5 had acute infectious or active inflammatory diseases, and 3 were healthy donors from the Etablissement Français du Sang. No significant differences were observed within this group (Table 2).

Detection of circulating KSHV$^+$ cells during MCD flares

Using multiparameter flow cytometry, we were able to detect a significant percentage of IgM$^+$CD38^{high} circulating cells showing an elevated forward scatter in 14 of 18 (78%) patients (Figure 1). The percentage of these cells varied between 0.16% and 2.54% after exclusion of T cells and monocytes (expressed in percent of CD3$^-$CD14$^-$ cells). Surface IgM was λ^+ in the 14 patients. CD24 was uniformly negative, pointing out that IgM$^+$CD38^{high} circulating cells were not transitional B cells. Further characterization showed that CD40, a pan–B-cell marker, was strongly decreased on the surface of these cells when compared with conventional B cells and plasmablasts (median of positive cells, 6%; IQR, 3%-11%; median MFI, 219) (Figures 1 and 2; supplemental Figure 3). The cells also had a heterogeneous expression of CD19 (median of positive cells, 24%; IQR, 15%-37%; median MFI, 613) and CD27 (median of positive cells, 24%; IQR, 11%-34%; median MFI, 701). A small fraction was CD20$^+$ (median of positive cells, 5%; IQR, 4% to 8%) (Figure 1 and Table 3). Interestingly, the 2 patients diagnosed with flare in the month after rituximab infusion had the same IgM$^+\lambda^+$CD38^{high}CD24$^-$ circulating population (7.3% and 0.6% of CD3$^-$CD14$^-$ cells, respectively). These cells were not found in KSHV$^+$ and KSHV$^-$ control populations. In the controls, IgM$^+$CD38^{high} circulating cells had a balanced κ/λ ratio and consisted in either transitional B cells (IgM$^+$CD38^{high}CD24$^+$CD40$^+$) or nonswitched plasmablasts (IgM$^+$CD38^{high}CD27^{high}CD40^{low}) (supplemental Figure 2).

The similar phenotype of IgM$^+\lambda^+$CD38^{high} circulating cells and KSHV$^+$ cells found in MCD lymph node[3,4] led us to explore their KSHV status. First, we performed immunofluorescence experiments, staining PBMCs with anti-LNA and anti-IgM antibodies (n = 1). An IgM/LNA costaining of large circulating cells was observed, arguing for KSHV infection of the IgM$^+\lambda^+$CD38^{high}CD24$^-$ population (supplemental Figure 4).

Next, we confirmed the infection of the circulating population using the flow-FISH method, which was previously used to identify EBV$^+$ cells in the setting of chronic active EBV infection.[11] This technique is based on the PrimeFlow RNA assay[11,12] and allows the detection of viral messenger RNAs and, in this study, the detection of a latent transcript, LNA, and a lytic transcript, vIL-6. We assessed the sensitivity of the target probes on the BCP1 cell line, a KSHV$^+$/EBV$^-$ PEL-derived cell line (supplemental Figure 5). LNA and vIL-6 probes proved highly sensitive because they both hybridized 90% of BCP1 cells (positive control hybridization RPL13A = 96%). They also proved to be highly specific because the number of LNA$^+$ and vIL-6$^+$ cells in KSHV$^-$ control PBMCs (n = 6) and EBV$^+$ lymphoblastoid cell line was comparable with the background observed with the negative control *Bacillus* probe (supplemental Figure 5). Subsequently, we examined the blood samples of 6 patients with KSHV-MCD flare who had detectable IgM$^+\lambda^+$CD38^{high}CD24$^-$ circulating cells. All patients showed KSHV$^+$ circulating cells among CD3$^-$CD14$^-$ cells, most of them corresponding to the IgM$^+\lambda^+$CD38^{high}CD24$^-$ population (Figure 3). A few KSHV$^+$ CD3$^-$CD14$^-$ cells were IgM$^-$ and/or CD38$^-$, especially in patients 1, 5, and 6 (Figure 3). They had a low MFI of LNA and vIL-6 when compared with the KSHV$^+$IgM$^+$CD38$^+$ population and to the KSHV$^+$EBV$^-$ PEL cell line BCP-1, indicating that this population might be related to nonspecific staining. Further studies using additional markers will be needed to demonstrate the true nature of this IgM$^-$CD38$^-$ population. All samples had an excellent hybridization quality, as shown by *Bacillus* (bacterial RNA, negative control) and RPL13A (ubiquitous ribosomal RNA expressed in all human cell types, positive control) hybridizations (supplemental Figure 6).

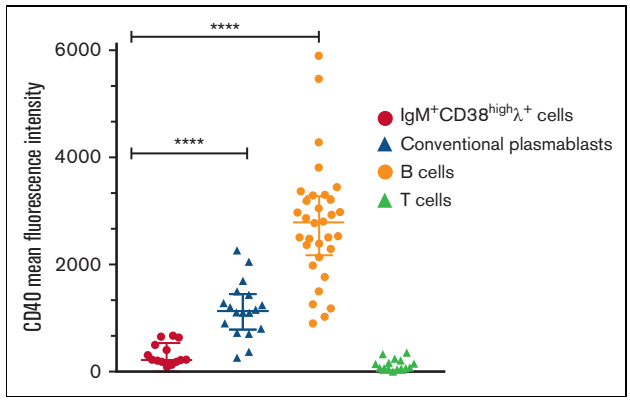

Figure 2. Low CD40 surface expression on circulating IgM$^+\lambda^+$CD38^{high} cells during KSHV-MCD flare. MFI is normalized on isotype MFI (MFI = CD40 MFI-isotype MFI) and expressed for KIV, conventional plasmablasts, and B and T cells. Median values and IQRs are represented for each plot. ****$P < .0001$, Mann-Whitney U test.

KSHV$^+$ cells harbor a distinct phenotype from conventional plasmablasts and display low expression of costimulatory molecules

Pathologists originally described LNA$^+$ large cells within KSHV-MCD lymph nodes and named them plasmablasts, giving birth to the plasmablastic variant of MCD. Conventional plasmablasts are uniformly CD19^{low}CD27^{high}CD38^{high} and are mostly isotype switched. Plasmablasts are detected within 2 weeks after infection or vaccination and may also expand in patients with active autoimmune diseases.[13,14] To compare the phenotype of KSHV$^+$ cells and that of conventional plasmablasts, we recruited participants after severe acute respiratory syndrome coronavirus 2 vaccination

Downloaded from http://ashpublications.net/bloodadvances/article-pdf/7/9/1682/2049158/blooda_adv-2022-008456-main.pdf by guest on 08 June 2024

Table 3. Summary of the surface phenotype of KIV and conventional plasmablasts

	KIVs	Conventional plasmablasts
CD19	Heterogeneous (~25% positivity)	Uniformly low
CD20	Heterogeneous (~5% positivity)	Negative
CD38	100% high positivity	100% high positivity
IgM	100% high positivity	Heterogeneous (~20% positivity)
κ/λ	Monotypic λ (100% high positivity)	Balanced κ/λ ratio (60/40%)
CD27	Heterogeneous (~25% positivity)	100% high positivity
CD40	Low/negative	Heterogeneous
CD70	Heterogeneous (6% positivity)	Negative
CD86	Heterogeneous (10% positivity)	Mostly positive
CD137L	Negative	Negative
OX40-L	Negative	Negative
ICOS-L	Negative	Negative
BAFF-R	Negative	Negative
PD-L1	Negative	Negative

(n = 13; 11 prime and 2 boosts, all with messenger RNA vaccines), viral primary infections (EBV and HIV, 1 of each condition), acute malaria (n = 1), and during systemic lupus erythematosus and IgG4-related disease flares (1 of each condition) (listed in Table 2). All had circulating $CD19^{low}CD27^{high}CD38^{high}$ conventional plasmablasts varying between 0.01% and 26% of $CD3^{-}CD14^{-}$ cells. These plasmablasts were mainly isotype switched (median of IgM^{-} plasmablasts, 81%; IQR, 69% to 87%), with a balanced κ/λ ratio and uniformly expressed CD27. CD40 MFI was significantly lower in $KSHV^{+}$ cells compared with plasmablasts (Figures 2 and 4; supplemental Figure 2). Altogether, these data indicate that despite a plasmablastic-like morphology, $KSHV^{+}$ cells show a singular phenotypic signature, and we propose to rename these cells KSHV-infected viroblasts (KIVs).

The expression of the costimulatory molecules involved in T-cell synapse and activation was assessed on KIV to explore their immunogenicity. They had a low and heterogeneous expression of CD70 (6%; IQR, 3%-9%; n = 4) and CD86 (9%; IQR, 8%-12%; n = 4) and no expression of CD137L (n = 2), OX40-L (n = 4), ICOS-L (n = 4), and BAFF-R (n = 2) (summarized in Table 3 and Figure 4). These data contrasted with the costimulatory profile of 2 virally transformed cell lines (EBV^{+} LCL and $KSHV^{+}EBV^{-}$ BCP1 cell line), underlying the low immunogenic phenotype of KIV. However, the transformed nature of the virally infected controls needs to be integrated in the interpretation of the data. PD-L1, a potential therapeutic target, was not expressed on KIV (n = 4). The expression of CD86 appeared as an excellent marker to differentiate KIV from conventional plasmablasts with a significantly higher expression on the latter (Figure 4). Interestingly, the BCP1 cell line also lacked CD40 expression, a finding that could point toward a virally induced decrease of CD40 surface expression (Figure 4).

KIV do not produce hIL-6 but produce IL-10

KSHV-MCD flares are characterized by clinical and biological features of systemic inflammation. Previous reports demonstrated that, during flares, high levels of hIL-6 and hIL-10 were detected in patient sera.[1] To explore the contribution of KIV to the cytokine release, we performed hIL-6 and hIL-10 intracellular staining on PBMCs from 3 patients (P1, P3, and P7) sampled during a KSHV-MCD flare. The production of hIL-6 was attributed to monocytes because 15%, 18%, and 47% of monocytes in P1, P3, and P7, respectively, were $hIL\text{-}6^{+}$, whereas KIVs were not $hIL\text{-}6^{+}$. Interestingly, a high proportion of KIV were $hIL\text{-}10^{+}$ (39%, 45%, and 78%, respectively), whereas T cells, B cells, and monocytes were $IL\text{-}10^{-}$ (Figure 5). These findings underline a cytokine signature of KIV beyond their phenotypic singularity.

Discussion

This study reports the detection of circulating KSHV-infected cells or KIV in patients with active KSHV-MCD. Circulating KIV harbor the same phenotype as $KSHV^{+}$ plasmablasts described in the mantle zone of lymph nodes of patients with KSHV-MCD.[3-5,15,16] This circulating $IgM^{+}\lambda^{+}CD38^{high}CD24^{-}$ population was identified in 78% of patients with disease flare and was absent from $KSHV^{+}$ and $KSHV^{-}$ control samples. The same cells were observed in 2 patients with postrituximab MCD flares. The absence of KIV detection during KSHV-MCD flares was associated with recent exposure to high-dose steroids (n = 1) and/or etoposide (n = 1). Freezing or delay in PBMC isolation was also found to substantially decrease the percentage of KIV (data not shown), and we advise rapid analysis (<6 hours) of blood samples to allow proper KIV identification. Moreover, other KSHV-related conditions need to be tested to assess the specificity of the technique. The immunophenotype of $KSHV^{+}$ DLBCL with lack of B-cell markers, expression of λ light chain, and expression of CD38 and MUM1 is not dissimilar from the KIV described in KSHV-MCD.[17] It would be interesting to study this population in the future and to look at surface markers that might be differentially expressed between $KSHV^{+}$ MCD and KSHV DLBCL. Another rare entity associated with KSHV is the KSHV-associated inflammatory cytokine syndrome, which, although not a lymphoproliferative disorder, has several clinical, radiological, and virological similarities with KSHV-MCD. Patients with KSHV-associated inflammatory cytokine syndrome have high human herpesvirus 8 viremia and elevated systemic levels of hIL-6, vIL-6, and hIL-10[18]. This specific $KSHV^{+}$ population lacking overt lymphoproliferative disorder would also be of particular interest of study, as some circulating KSHV-infected cells might be detected in these patients. In conclusion, more data are needed to better define this test's positive and negative predictive value and the exact clinical significance of KIV detection in the diagnosis of KSHV-MCD. KIV detection could add some additional weight when suspecting KSHV-MCD and waiting for the results of a lymph node biopsy. As for whole-blood KSHV DNA viral load, KIV detection raises the possibility of $KSHV^{+}$ MCD flare but does not confirm the diagnosis.

The detection of circulating KIV allowed us to better characterize the phenotype of $KSHV^{+}$ cells during MCD using multicolor flow cytometry. We first compared KIV with conventional plasmablasts found during infectious or autoimmune diseases. Despite similar aspects in size and granularity, analysis of cell surface markers showed that KIV were uniformly IgM^{+} with a λ monotypic restriction profile and a partial expression of the CD19 and CD20 B-cell markers. Moreover, these cells partially expressed the costimulatory molecule CD27, with very low or lack of CD40 expression. These results indicate that $KSHV^{+}$ cells found in MCD should be better

Downloaded from http://ashpublications.net/bloodadvances/article-pdf/7/9/1682/2049158/blooda_adv-2022-008456-main.pdf by guest on 08 June 2024

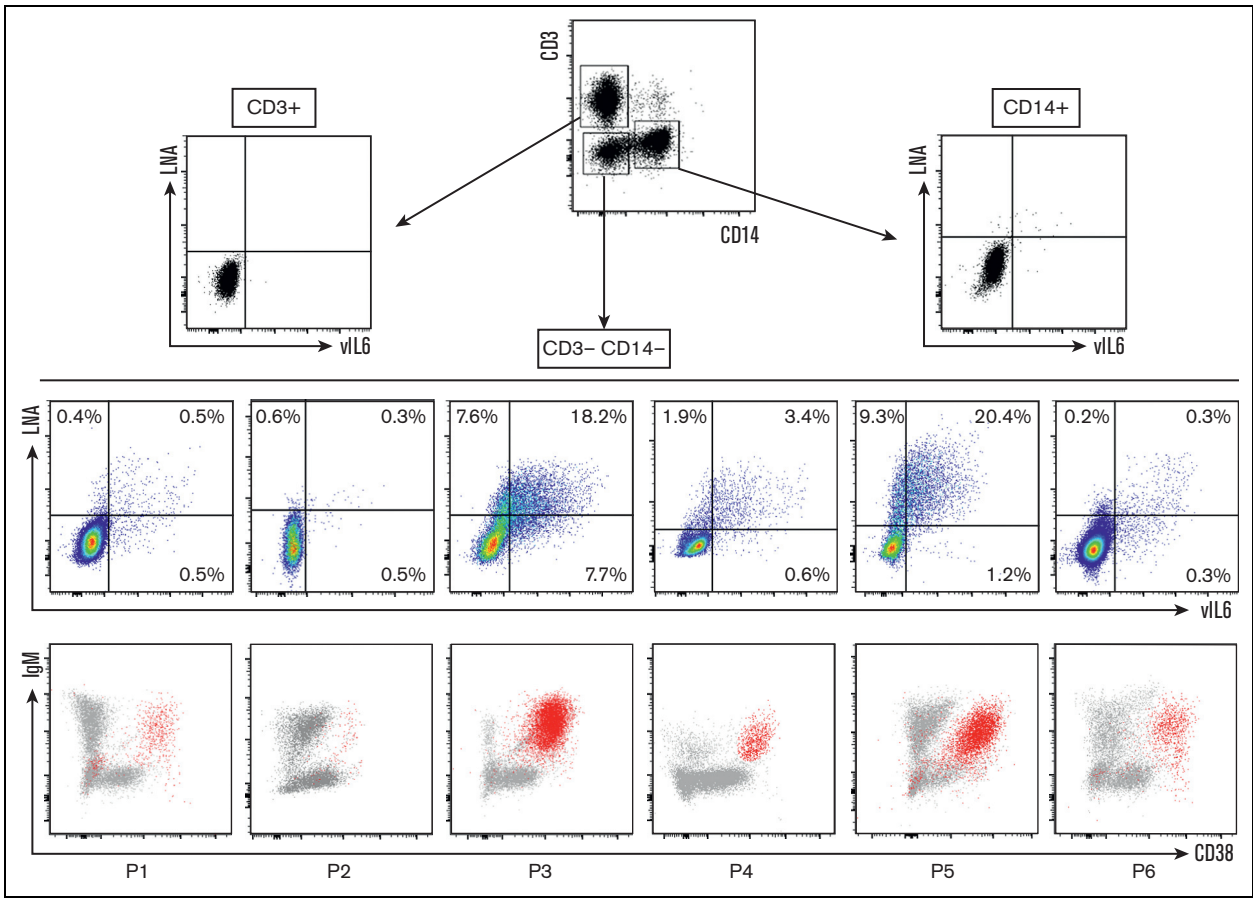

Figure 3. Identification of circulating KIV during KSHV-MCD flare using LNA/vIL-6 flow-FISH. Flow-FISH was performed on the peripheral blood of 6 patients with confirmed KSHV-MCD flare. LNA$^+$ and/or vIL-6$^+$ cells are represented among CD3$^+$ (T cells), CD14$^+$ (monocytes), and CD3$^-$CD14$^-$ cells. Values are given as percentages of positive cells among CD3$^-$CD14$^-$ cells. LNA$^+$ and/or vIL-6$^+$ cells are depicted in red in an IgM/CD38 dot plot for each patient, showing that most of the infected cells are IgM$^+$ and CD38$^+$ cells.

designated as KIVs rather than plasmablasts because of their strong phenotypical differences. This peculiar population found during KSHV-MCD flare appears to be driven by KSHV infection and does not correspond to a reactive postinfectious population.

Variability in CD20, CD27, and CD70 expression within KIV led us to hypothesize that KSHV could infect multiple cellular subtypes. Whether KSHV directly infects multiple B-cell or plasma cell populations or only a CD20$^+$ precursor B cell during MCD is currently unknown. An in vitro infection model favors the latter hypothesis, because KIV could be obtained after infection of tonsillar naïve B cells.[19] This could also explain why rituximab, an anti-CD20 antibody, is highly effective in KSHV-MCD, acting through a rapid depletion of the CD20$^+$ B-cell population targeted by KSHV. Of note, we failed to identify any correlation between CD20 expression and responsiveness to rituximab. Additional studies are required to further characterize KSHV-infected populations during MCD flares and connect host cellular subtypes to viral programs.

One striking feature was the substantial decrease of CD40 on KIV, in contrast with other B-cell populations. CD40 is a costimulatory molecule expressed on B cells engaging with CD40 ligand present on activated T cells, leading to isotype-switch induction and somatic hypermutation.[20] Patients that are CD40 deficient[21] experience hyper IgM syndrome, a primary immunodeficiency characterized by a defect in isotype-switched memory B cells, with only IgM$^+$ and naïve B cells. These data suggest that CD40 deficiency could prevent affinity maturation and account for the IgM$^+$ and immunoglobulin-unmutated phenotype observed in the infected cells.[3] The lack of CD40 expression was also found in the BCP1 cell line, whereas the EBV$^+$ LCL expressed CD40. This finding could point toward a KSHV-induced decrease in CD40 expression. The strong reduction in CD40 expression led us to further assess the expression of other costimulatory molecules involved in the T-cell synapse. KIV showed an overall decrease of CD27, CD40, CD70, CD86, CD137L, OX40-L, BAFF-R, and ICOS-L. Costimulation defects might participate in KSHV-MCD emergence because monogenic defects in the CD27-CD70 axis are associated with susceptibility to EBV,[22] another herpesvirus, and a monogenic defect in OX40 has been described in a child with early-onset KS.[23] The overall weak costimulatory profile of KIV might play a role in T-cell immune escape during MCD. Moreover, KIV-restricted IL-10 production may also participate in the immune escape of KSHV. IL-10 is an anti-inflammatory cytokine that KSHV might use to create a tolerogenic environment around KIV, especially in secondary lymphoid organs, to replicate and escape from T-cell cytotoxicity. Interestingly, murine gammaherpesvirus

Downloaded from http://ashpublications.net/bloodadvances/article-pdf/7/9/1682/2049158/blooda_adv-2022-008456-main.pdf by guest on 08 June 2024

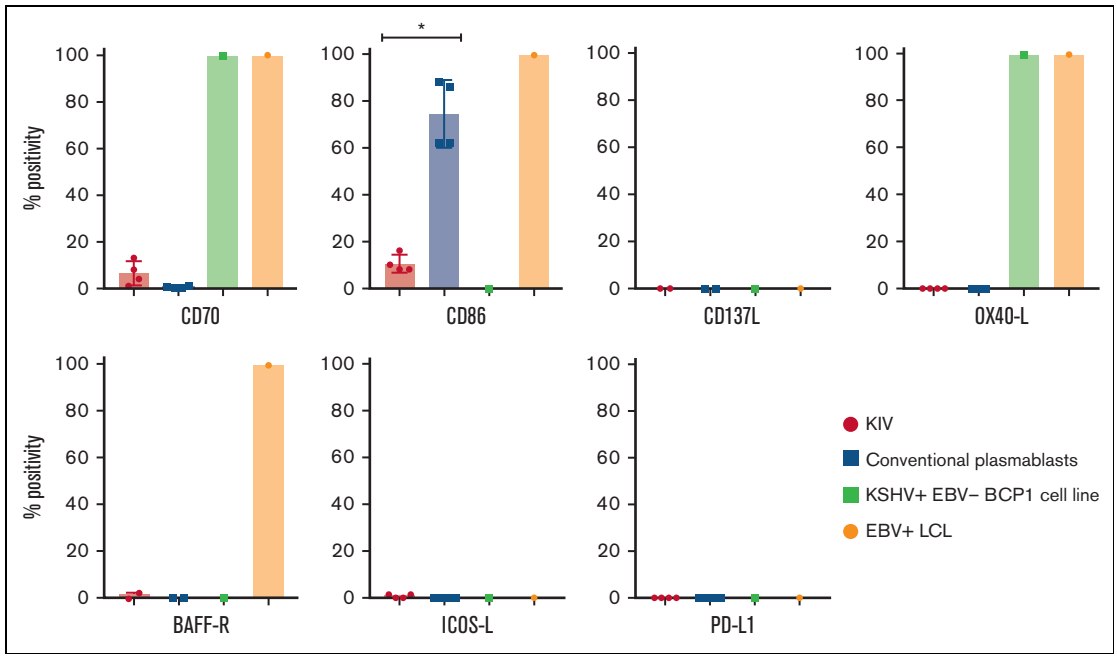

Figure 4. Surface expression of costimulatory molecules on KIV, conventional plasmablasts, KSHV$^+$EBV$^-$ BCP1 cell line, and EBV$^+$ LCL. Histograms represent the percentage of CD40$^+$, CD70$^+$, CD86$^+$, CD137L$^+$, OX40-L$^+$, BAFF-R$^+$, ICOS-L$^+$, and PD-L1$^+$ cells among KIV, conventional plasmablasts, KSHV$^+$EBV$^-$ BCP1 cell line and EBV$^+$ LCL. The number of samples tested for each marker is detailed in the manuscript. *$P < .05$, Mann-Whitney U test.

68 similarly induces murine IL-10 production by host B cells. In this murine model, viral latency establishment and B-cell survival, proliferation, and differentiation to preplasma cells are IL-10 dependent.[24] A similar role of IL-10 in the pathophysiology of KSHV-MCD needs to be investigated in the future. Besides vIL-6 production by KIV, KSHV replication also triggers hIL-6 production by monocytes, suggesting a potential effect of anti–IL-6 receptors in KSHV-MCD, as in other viral infections.[25] Anti–IL-6 receptor therapies have been tested in KSHV-MCD with a transient clinical response but quick relapse and persistent elevated IL-10 blood levels and KSVH viral load throughout the treatment.[26] These clinical findings do not support a key role of hIL-6 in viral persistence. Targeting the IL-10 pathway could be an attractive therapeutic option in KSHV-MCD. KSHV-MCD is frequently encountered in immunocompromised

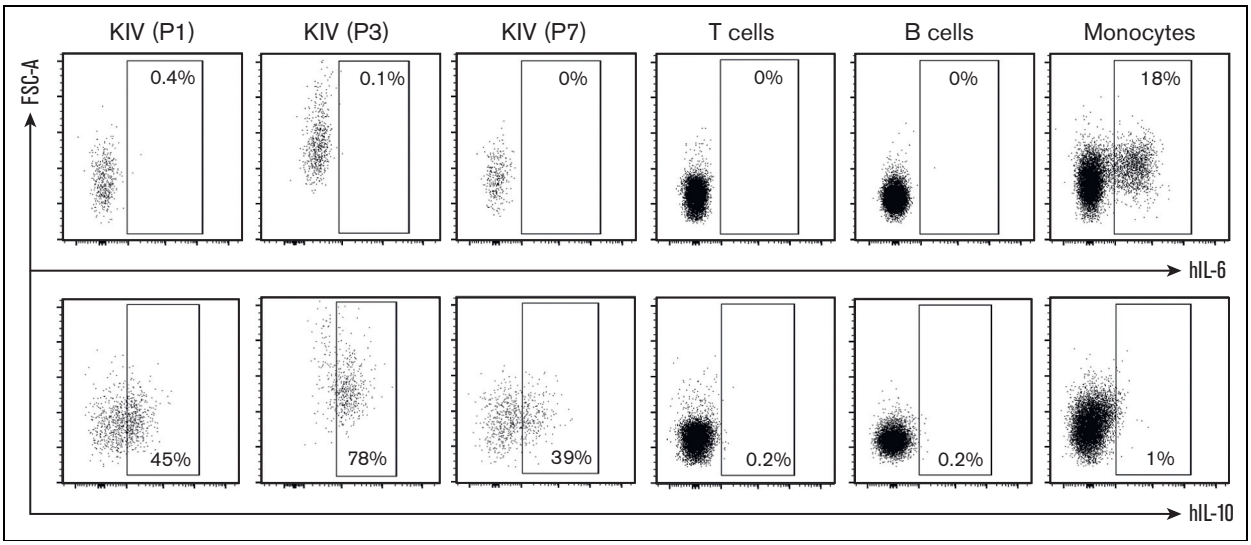

Figure 5. hIL-6 and hIL-10 intracellular staining on PBMCs from 3 patients with KSHV-MCD flare. PBMCs were left unstimulated and intracellular detection of hIL-6 (top) and hIL-10 (bottom) was assessed in KIV, T cells, B cells, and monocytes. KIV staining is shown for the 3 patients (P1, P3, and P7), whereas staining of T cells, B cells, and monocytes is only shown for 1 representative patient (P1) for the purpose of clarity. hIL-6 and hIL-10 staining was negative in B cells and T cells from the 3 patients tested, whereas P3 and P7 had 15% and 47%, respectively, IL-6$^+$ monocytes.

Downloaded from http://ashpublications.net/bloodadvances/article-pdf/7/9/1682/2049158/blooda_adv-2022-008456-main.pdf by guest on 08 June 2024

hosts, but the exact nature of the immune deficiency leading to MCD emergence is unknown. Of note, only 50% of patients in this study were infected with HIV, and the other half did not have a known cause of immunodeficiency. T-cell repertoire appears to be functional and polyreactive in patients with KSHV-MCD,[27] but cell-to-cell experiments have not been assessed; they could provide further insights into the understanding of KSHV-MCD pathophysiology. This could be addressed using easy access to KIV in the peripheral blood of patients with active KSHV-MCD. The findings reported herein give additional information to a previous study by our group that focused on the T-cell aspect of KSHV-MCD pathophysiology, which showed that a decrease in the number of invariant natural killer T cells might be involved in a defective control of KSHV-promoting KIV expansion.[28] This study focuses on the B-cell aspect of KHSV-MCD and shows how KIV phenotype could promote immune escape from T-cell surveillance by down-regulation of costimulatory molecules and secretion of suppressive cytokines. Immune defects involved in KSHV-MCD appear to affect multiple components of the immune system, making the pathophysiology of KSHV-MCD a multistep and complex process.

Acknowledgments

The authors thank Niclas Setterblad from the Institut Universitaire d'Hématologie platform, Hôpital Saint-Louis, Paris, France for confocal microscopy assistance; the Etablissement Français du Sang (EFS, Hôpital Saint-Louis, Paris, France) for providing control samples; and Fabien Touzot for careful critical reading of the manuscript.

This work was funded by French National Agency for Research on AIDS and Viral Hepatitis and by the French National Reference Centre for Castleman Disease (Hôpital Saint-Louis, Paris, France).

Authorship

Contribution: G.M.d.F., A.V., and D.B. wrote the manuscript; G.M.d.F., A.V., M.G., A.D., L.G., R.B., E.F., C.L., A.M.R., E.O., and D.B. contributed to the patient recruitment and management; G.M.d.F., A.V., S.K., Z.S., M.C., A.D., J.P., M.-A.S., and D.B. performed the experiments; G.M.d.F., A.V., S.K., B.F., M.-A.S., S.L., E.O., G.C., and D.B. analyzed the data; J.L.G. and M.S. performed whole-blood KSHV quantification; V.M. performed pathological reviewing of MCD samples; A.V. designed the graphical abstract; D.B. and G.C. supervised the project; and all authors critically reviewed the manuscript.

Conflict-of-interest disclosure: E.O. is a consultant for EUSA Pharma. The remaining authors declare no competing financial interests.

ORCID profiles: A.V., 0000-0002-9288-3386; Z.S., 0000-0002-6695-7695; B.F., 0000-0002-4189-996X; A.D., 0000-0002-2008-2942; J.V., 0000-0002-6601-7820; L.G., 0000-0002-0360-7620; M.S., 0000-0001-7985-6132; E.F., 0000-0002-3707-0278; C.C., 0000-0002-5087-4414; S.L., 0000-0001-8238-4391; E.O., 0000-0001-8588-7138; D.B., 0000-0002-5006-8279.

Correspondence: David Boutboul, Department of Clinical Immunology, Hôpital Saint-Louis, Assistance Publique-Hôpitaux de Paris (AP-HP), Université de Paris Cité, 1 Ave Claude Vellefaux, 75010 Paris, France; email: david.boutboul@aphp.fr.

References

1. Oksenhendler E, Carcelain G, Aoki Y, et al. High levels of human herpesvirus 8 viral load, human interleukin-6, interleukin-10, and C reactive protein correlate with exacerbation of multicentric castleman disease in HIV-infected patients. *Blood*. 2000;96(6):2069-2073.
2. Oksenhendler E, Boutboul D, Fajgenbaum D, et al. The full spectrum of Castleman disease: 273 patients studied over 20 years. *Br J Haematol*. 2018;180(2):206-216.
3. Dupin N, Diss TL, Kellam P, et al. HHV-8 is associated with a plasmablastic variant of Castleman disease that is linked to HHV-8–positive plasmablastic lymphoma. *Blood*. 2000;95(4):1406-1412.
4. Du MQ, Liu H, Diss TC, et al. Kaposi sarcoma-associated herpesvirus infects monotypic (IgM lambda) but polyclonal naive B cells in Castleman disease and associated lymphoproliferative disorders. *Blood*. 2001;97(7):2130-2136.
5. Chadburn A, Hyjek EM, Tam W, et al. Immunophenotypic analysis of the Kaposi sarcoma herpesvirus (KSHV; HHV-8)-infected B cells in HIV+ multicentric Castleman disease (MCD). *Histopathology*. 2008;53(5):513-524.
6. Marcelin A, Motol J, Guihot A, et al. Relationship between the quantity of Kaposi sarcoma–associated herpesvirus (kshv) in peripheral blood and effusion fluid samples and KSHV-associated disease. *J Infect Dis*. 2007;196(8):1163-1166.
7. Sayer R, Paul J, Tuke PW, et al. Can plasma HHV8 viral load be used to differentiate multicentric Castleman disease from Kaposi sarcoma? *Int J STD AIDS*. 2011;22(10):585-589.
8. Gérard L, Bérezné A, Galicier L, et al. Prospective study of rituximab in chemotherapy-dependent human immunodeficiency virus–associated multicentric Castleman's disease: ANRS 117 CastlemaB Trial. *JCO*. 2007;25(22):3350-3356.
9. Bower M, Newsom-Davis T, Naresh K, et al. Clinical features and outcome in HIV-associated multicentric Castleman's disease. *JCO*. 2011;29(18):2481-2486.
10. Oksenhendler E, Boutboul D, Beldjord K, et al. Human herpesvirus 8+ polyclonal IgMλ B-cell lymphocytosis mimicking plasmablastic leukemia/lymphoma in HIV-infected patients. *Eur J Haematol*. 2013;91(6):497-503.
11. Fournier B, Boutboul D, Bruneau J, et al. Rapid identification and characterization of infected cells in blood during chronic active Epstein-Barr virus infection. *J Exp Med*. 2020;217(11):e20192262.

Downloaded from http://ashpublications.net/bloodadvances/article-pdf/7/9/1682/2049158/blooda_adv-2022-008456-main.pdf by guest on 08 June 2024

12. Henning AL, Sampson JNB, McFarlin BK. Measurement of low-abundance intracellular mRNA using amplified FISH staining and image-based flow cytometry. *Current Protocols in Cytometry*. 2016;76(1).
13. Wallace ZS, Mattoo H, Carruthers M, et al. Plasmablasts as a biomarker for IgG4-related disease, independent of serum IgG4 concentrations. *Ann Rheum Dis*. 2015;74(1):190-195.
14. Carter MJ, Mitchell RM, Meyer Sauteur PM, Kelly DF, Trück J. The antibody-secreting cell response to infection: kinetics and clinical applications. *Front Immunol*. 2017;8:630.
15. Katano H, Sato Y, Kurata T, Mori S, Sata T. Expression and localization of human herpesvirus 8-encoded proteins in primary effusion lymphoma, Kaposi's Sarcoma, and multicentric Castleman's disease. *Virology*. 2000;269(2):335-344.
16. Parravicini C, Corbellino M, Paulli M, et al. Expression of a virus-derived cytokine, KSHV vIL-6, in HIV-seronegative Castleman's disease. *Am J Pathol*. 1997;151(6):1517-1522.
17. Oksenhendler E, Boutboul D, Galicier L. Kaposi sarcoma-associated herpesvirus/human herpesvirus 8-associated lymphoproliferative disorders. *Blood*. 2019;133(11):1186-1190.
18. Polizzotto MN, Uldrick TS, Wyvill KM, et al. Clinical features and outcomes of patients with symptomatic Kaposi sarcoma herpesvirus (KSHV)-associated inflammation: prospective characterization of KSHV inflammatory cytokine syndrome (KICS). *Clin Infect Dis*. 2016;62(6):730-738.
19. Aalam F, Nabiee R, Castano JR, Totonchy J. Analysis of KSHV B lymphocyte lineage tropism in human tonsil reveals efficient infection of CD138+ plasma cellsTarakanova VL, ed. *PLoS Pathog*. 2020;16(10):e1008968.
20. Laman JD, Claassen E, Noelle RJ. Functions of CD40 and its ligand, gp39 (CD40L). *Crit Rev Immunol*. 2017;37(2-6):371-420.
21. DiSanto JP, Bonnefoy JY, Gauchatt JF, Fischer A, Saint Basile G de. CD40 ligand mutations in X-linked immunodeficiency with hyper-IgM. *Nature*. 1993;361(6412):541-543.
22. Latour S, Fischer A. Signaling pathways involved in the T-cell-mediated immunity against Epstein-Barr virus: lessons from genetic diseases. *Immunol Rev*. 2019;291(1):174-189.
23. Byun M, Ma CS, Akçay A, et al. Inherited human OX40 deficiency underlying classic Kaposi sarcoma of childhood. *J Exp Med*. 2013;210(9):1743-1759.
24. Siegel AM, Herskowitz JH, Speck SH. The MHV68 M2 protein drives IL-10 dependent B cell proliferation and differentiationSugden B, ed. *PLoS Pathog*. 2008;4(4):e1000039.
25. The REMAP-CAP Investigators. Interleukin-6 receptor antagonists in critically ill patients with Covid-19. *N Engl J Med*. 2021;384(16):1491-1502.
26. Ramaswami R, Lurain K, Peer CJ, et al. Tocilizumab in patients with symptomatic Kaposi sarcoma herpesvirus–associated multicentric Castleman disease. *Blood*. 2020;135(25):2316-2319.
27. Guihot A, Oksenhendler E, Galicier L, et al. Multicentric Castleman disease is associated with polyfunctional effector memory HHV-8–specific CD8+ T cells. *Blood*. 2008;111(3):1387-1395.
28. Sbihi Z, Dossier A, Boutboul D, et al. iNKT and memory B-cell alterations in HHV-8 multicentric Castleman disease. *Blood*. 2017;129(7):855-865.

Downloaded from http://ashpublications.net/bloodadvances/article-pdf/7/9/1682/2049158/blooda_adv-2022-008456-main.pdf by guest on 08 June 2024